Self-assembled polymeric vectors mixtures: characterization of the polymorphism and existence of synergistic effects in photodynamic therapy

Ugo Till, Laure Gibot, Christophe Mingotaud, Patricia Vicendo, Marie-Pierre Rols, Mireille Gaucher, Frédéric Violleau, Anne-Françoise Mingotaud

doi:10.1088/0957 4484/27/31/315102

Self-assembled polymeric vectors mixtures: characterization of the polymorphism and existence of synergistic effects in photodynamic therapy

Ugo Till[1,2], Laure Gibot[3], Christophe Mingotaud[2], Patricia Vicendo[2], Marie-Pierre Rols[3], Mireille Gaucher[1], Frédéric Violleau[4] and Anne-Françoise Mingotaud[2]

[1] Université de Toulouse, Institut National Polytechnique de Toulouse Ecole d'Ingénieurs de Purpan, Département Sciences Agronomiques et Agroalimentaires, 75 voie du TOEC, BP 57611, F 31076 Toulouse Cedex 03, France
[2] Laboratoire des IMRCP, Université de Toulouse, CNRS UMR 5623, Université Paul Sabatier, 118 route de Narbonne, F 31062, Toulouse Cedex 9, France
[3] Institut de Pharmacologie et de Biologie Structurale, Université de Toulouse, CNRS, UPS, France
[4] Laboratoire de Chimie Agro industrielle (LCA), Université de Toulouse, INRA, INPT, INP EI PURPAN, Toulouse, France

E mail: afmingo@chimie.ups tlse.fr and frederic.violleau@purpan.fr

Abstract

The objective of this work was to assess the relation between the purity of polymeric self-assemblies vectors solution and their photodynamic therapeutic efficiency. For this, several amphiphilic block copolymers of poly(ethyleneoxide-b-ε-caprolactone) have been used to form self-assemblies with different morphologies (micelles, worm-like micelles or vesicles). In a first step, controlled mixtures of preformed micelles and vesicles have been characterized both by dynamic light scattering and asymmetrical flow field flow fractionation (AsFlFFF). For this, a custom-made program, STORMS, was developed to analyze DLS data in a thorough manner by providing a large set of fitting parameters. This showed that DLS only sensed the larger vesicles when the micelles/vesicles ratio was 80/20 w/w. On the other hand, AsFlFFF allowed clear detection of the presence of micelles when this same ratio was as low as 10/90. Subsequently, the photodynamic therapy efficiency of various controlled mixtures was assessed using multicellular spheroids when a photosensitizer, pheophorbide a, was encapsulated in the polymer self-assemblies. Some mixtures were shown to be as efficient as monomorphous systems. In some cases, mixtures were found to exhibit a higher PDT efficiency compared to the individual nano-objects, revealing a synergistic effect for the efficient delivery of the photosensitizer. Polymorphous vectors can therefore be superior in therapeutic applications.

S Online supplementary data available from stacks.iop.org/NANO/27/315102/mmedia

Keywords: polymeric micelles, vesicles, polymersomes, self-assembly, asymmetrical flow field flow fractionation, photodynamic therapy, spheroids

(Some figures may appear in colour only in the online journal)

1. Introduction

With the development of controlled polymerization processes, polymer engineering has really exploded over the last 20 years. The use of either ring-opening or controlled radical polymerization enables in simple conditions the formation of polymer structures with various backbones such as aliphatic polyesters or polyacrylates. In parallel with this, the discovery of the enhanced permeability and retention effect (EPR) by Maeda and Matsumura [1] in the late 80s has further resulted in the exploration of all these structures as nanovectors in the field of nanomedicine in oncology [2 7]. The EPR effect is linked to the presence of cellular disjunctions on the endothelial cells in the vicinity of tumors that lead to the extravasation of nano-objects from the bloodstream and their favored retention due to a lack of efficient lymphatic system in the tumors. This results in a passive targeting of 15 200 nm range nano-objects towards a majority of tumors, therefore offering the possibility to modify the biodistribution of anticancer drugs, the toxicity of which is responsible for severe side effects. Among the numerous studies dealing with polymeric nanovectors for cancer treatment, the outline is very similar for all publications: formation of the assemblies, characterization by dynamic light scattering (DLS) and transmission electron microscopy (TEM), characterization of the encapsulation of the drug and its release, *in vitro* cytotoxicity and possibly *in vivo* experiments to prove the better efficiency of the encapsulated system. In most cases, studies try to use 'well-defined' self-assemblies, meaning that a single population of nano-objects is looked for, with varying polydispersity. However, the use of only DLS and TEM techniques might be misleading. Indeed, DLS provides an analysis of the solution in its whole and, if present, several populations might not be properly visible. TEM only shows a small portion of the solution and furthermore implies drying it. In some cases, cryo-TEM can be used to avoid drying [8], but this remains a difficult technique to master in order to avoid freezing artefacts and assemblies approaching the thickness of the ice cannot be analyzed correctly. In order to provide a better characterization of the nanovector solutions, we suggested the use of asymmetrical flow field flow fractionation (AsFlFFF) and showed that this technique was powerful to analyze all populations of self-assemblies possibly present in the solution [9 12]. By using this approach, we therefore aimed at answering the original question: are well-defined vectors better for nanomedicine or can controlled mixtures provide a similar activity or even a synergy to enable a better therapeutic efficiency? To the best of our knowledge, no study has so far assessed the issue of nanovectors' purity, as opposed for instance to their shape, which is increasingly examined [13 15].

Photodynamic therapy (PDT) uses a photosensitizer which is injected into the patient and subsequently irradiated to produce reactive oxygen species that kill the cells [16]. This approach has been known for over 30 years and is clinically used in the treatment of several oncologic [17] and ophthalmic diseases [18]. Nowadays, the use of PDT has been approved for clinical treatments in the USA, EU, Canada, Russia and Japan. The FDA approved the use of PDT in Barrett´s oesophagitis, obstructive tracheobroncheal carcinoma using the photosensitizer porfimer sodium (®Photofrin), and the use of 5-aminolevulinic acid, 5-ALA (®Levulan, ®Kerastick) for actinic keratosis while verteporfrin (®Visudyne) may be applied for macular degeneration. In addition to the above, the EU also approved the use of *meta*-tetrahydroxy-phenyl chlorin (mTHPC, ®Foscan) for the palliative treatment of advanced cases of head and neck carcinomas. The strong asset of this technique is the possibility to irradiate only the area to be treated. However, the biodistribution of the photosensitizer is not selective and the patient thus remains photosensitive for several days and has to avoid sun exposure. Interestingly, encapsulating the photosensitizer in nanovectors has been shown to avoid this general sensitization by a modification of the biodistribution in favor of the tumor by the EPR effect [19, 20] and has thus been studied for over a decade [16, 21], mainly in liposomes, polymer or silica nanoparticles and only in a few cases in polymer self-assemblies [11, 22 27]. Therefore, in this study, we first describe the encapsulation of an already validated photosensitizer, namely Pheophorbide a (Pheo), in different polymer self-assemblies of distinct shapes. These are subsequently used in mixtures of preformed nanovectors to assess PDT efficiency in 3D tumor models and thereby answer the central question of this work.

2. Materials and methods

2.1. Chemicals

All poly(ethyleneoxide-b-ε-caprolactone) (PEO-PCL) copolymers were bought from Polymer Source Inc. (Dorval Montréal, Canada), Pheo from Wako (Osaka, Japan). Different polymers were used with different molar masses which are mentioned in their denomination: PEO-PCL 5000-11000, PEO-PCL 5000-4000, PEO-PCL 2000-7000, PEO-PCL 2000-4800. PrestoBlue and cell culture medium were purchased from Invitrogen Life Technologies (Saint Aubin, France). Penicillin, streptomycin and PBS were from Sigma-Aldrich (Saint Quentin Fallavier, France). Ultrapure water was obtained from an ELGA Purelab Flex system (resistivity higher than 18.2 MΩ.cm) and was filtered on 0.2 μm RC filters just before use.

2.2. Polymersome formation by film rehydration

A 20 mg ml ^{1} polymer solution (PEO-PCL 5000-11000, PEO-PCL 2000-7000 or PEO-PCL 2000-4800) in chloroform was prepared and the solvent was evaporated on a rotary evaporator to form a regular film, which was further dried under vacuum for 4 h. The film was then rehydrated with 2 ml of milliQ water and heated at 65 °C for 30 min and at 65 °C for 1 h under sonication. The solution was then extruded on a mini-extruding system from Polar Avanti Lipids through a polycarbonate membrane with a cut-off of 0.4 μm.

2.3. Micelle preparation by the 'Acetone cosolvent' method

20 mg of PEO-PCL 5000-4000 were dissolved in 0.4 ml of acetone. This was added dropwise in 10 15 min to 5 ml ultrapure water under stirring. The solution was left standing for two days for acetone to evaporate.

2.4. Loading of the nano-objects with Pheo

For micelles, Pheo was added to the acetone solution during the preparation of the self-assemblies. For polymersomes, a 0.5 mg ml ^{1} Pheo solution in acetone was used and an adequate volume (80 160 μl depending on the system) added to the aqueous solution (2 ml) of polymersomes. The solution was left standing for two days to remove acetone. The chosen ratio of Pheo/polymer 1/30 mol mol ^{1} enabled us to obtain a full Pheo encapsulation, as shown in our earlier studies [10].

2.5. Mixture preparation

All nanovector stock solutions were used at a concentration of 5 mg ml ^{1}. The mixtures of nanovectors were made by mixing different volumes of the pure systems at ambient temperature. The resulting solution was stirred for one minute and characterized. The ratios presented throughout the manuscript are therefore either those of initial solution volumes or nanovector weight ratios. For the PDT experiments, the resulting solution was then further diluted in order to obtain the desired Pheo concentration.

2.6. Dynamic light scattering (DLS)

DLS was carried out at 25 °C on a Malvern (Orsay, France) Zetasizer NanoZS. Solutions were analyzed in triplicate without being filtered in order to characterize the plain samples. Data were analyzed by the general-purpose non-negative least squares (NNLS) method. The typical accuracy for these measurements was 10 20% for systems exhibiting a polydispersity index lower than 0.4.

The Malvern DLS data were further analyzed by a custom-made program named STORMS in order to obtain a more precise characterization of the solutions. This program has been designed with Matlab and enables the fitting of DLS correlograms using different sets of parameters, corresponding to all hypotheses that have to be made during the treatment. Indeed, going from correlograms to size results implies three levels of hypotheses: the first consisting in the transformation of autocorrelation data to diffusion coefficient, the second extracting the size of the scattering object from diffusion coefficient depending on its geometry, and finally using a model enabling the transformation of the intensity-relative population to a number-relative one. For each step, STORMS provides the choice of different parameters. For the nano-objects presented here, the protocol used a NNLS fitting, assumed a spherical shape for all objects, and the chosen scattering model was that corresponding to a mixture of micelles and vesicles (maximum micelle size fixed at a radius of 25 nm). Different sets of the range of decay rates and the regularization parameter were used, $\alpha = 5$, range $= 2$ being the default. Unless stated, this treatment provided residuals lower than 5×10^{3} for all analyses.

2.7. Transmission electron microscopy (TEM)

TEM experiments were performed with a Hitachi HT7700 microscope (accelerating voltage of 75 kV). Small amounts of particle suspensions in water were deposited onto a discharged copper grid coated with a carbon membrane and wiped with absorbent paper. A few drops of uranyl acetate solution were deposited onto the grid for 30 s, and the grid was then dried under a lamp for three minutes.

2.8. Asymmetrical flow field flow fractionation

The AsFlFFF instrument was an Eclipse 2 System (Wyatt Technology Europe, Dernbach, Germany). The AsFlFFF channel, designed with a 250 μm thick Mylar spacer had a trapezoidal shape with a length of 17.3 cm, an initial breadth of 1.65 cm, and a final breadth of 0.30 cm. The accumulation wall was an ultrafiltration membrane of regenerated cellulose with a 5 kDa cut-off (Wyatt Technology Europe, Dernbach, Germany). An Agilent 1100 Series Isocratic Pump (Agilent Technologies, Waldbronn, Germany) with an in-line vacuum degasser and an Agilent 1100 Autosampler delivered the carrier flow and handled sample injection into the AsFlFFF channel. A 0.1 μm in-line filter (VVLP, Millipore, Germany) was installed between the pump and the AsFlFFF channel. The products were detected with 18 angles Multi-Angle Light Scattering (MALS) DAWN-Heleos II (Wyatt Technology, Santa Barbara, CA, US), an Optilab Rex Refractometer (Wyatt Technology, Santa Barbara, CA, US), and a UV detector Agilent 1100 ($\lambda = 214$ nm or 412 nm). The MALS detectors were normalized with bovine serum albumin (BSA). Calibration of scattering intensity was performed with HPLC-grade filtered toluene. Water, which was filtered with 0.02% sodium azide before use, (vacuum filtration system using Gelman filters of 0.1 μm) was used as an eluent.

During focusing, the cross flow was fixed at 0.5 ml min ^{1}. After 1 min, 10 to 60 μl of sample were injected at 0.2 ml min ^{1} for two minutes. After injection, one minute of focus was maintained before the elution started. In elution mode, for the nano-object mixtures, the cross flow was first fixed to 0.4 ml min ^{1} for 20 min then changed over 5 min to 0.15 ml min ^{1} and kept constant for 25 min. For PEO-PCL 2000-4800, a 190 μm thick Mylar spacer was used and the cross flow rate was initially set to 0.5 ml min ^{1}. The cross flow rate then decreased linearly for 10 min to 0.15 ml min ^{1} and was maintained for 15 min. In all cases, cross flow was then stopped at the end of the elution period in order to eliminate all particles present in the AsFlFFF system.

2.9. Generation of tumor spheroids

Human HCT-116 and FaDu spheroids were produced by the non-adherent technique as previously described [28, 29]. Briefly, 10 000 FaDu head and neck cancer cells or 1 000 HCT-116 colorectal cancer cells in suspension were seeded in 300 μl of cell culture medium in ultra-low attachment 96-well

Table 1. Formation of polymer nano objects.

Polymer	Mn of PEO block (g mol^{-1})	Mn of hydrophobic block (g mol^{-1})	$f_{hydrophilic}$ [a] (%)	Preparation method
PEOPCL 2000 4800	2000	4800	29.4	Film rehydration
PEOPCL 2000 7000	2000	7000	22.2	Film rehydration
PEOPCL 5000 11 000	5000	11 000	31.2	Film rehydration
PEOPCL 5000 4000	5000	4000	55.5	Acetone cosolvent

[a] Weight fraction of hydrophilic part.

Table 2. DLS characterization of polymer self assemblies.

Polymer	D_H (nm) intensity average	D_H (nm) Number average	PDI	Morphology
PEOPCL 5000 11 000	100	88	0.25	vesicles
PEOPCL 5000 4000	28	22	0.17	micelles
PEOPCL 2000 7000	198	82	0.24	worm like systems

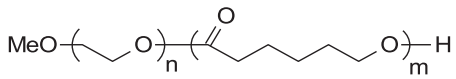

PEO-PCL

Scheme 1. PEO PCL chemical structure.

plates (Corning, Fisher Scientific, Illkirch, France). Spheroids were cultivated for 5 days before incubation with the nano-objects at 37 °C in a humidified atmosphere containing 5% CO_2.

2.10. Photodynamic therapy (PDT) of 3D tumor spheroids

Tumor spheroids were incubated 30 min with free or encapsulated Pheo 1 μM before the first illumination. Spheroids were then photo-irradiated for 8 min using an overhead projector lamp with a band-pass filter ($\lambda > 400$ nm). The total energy received was 8.2 J cm ^{2} for the 8 min duration. Then, 8 min illuminations were performed at 24 h intervals over three days. Spheroids treated by photodynamic therapy were observed 6 h after the last illumination by optical microscopy (Olympus BX53 equipped with a x5M plane N objective in phase contrast). Optical observation took place over three days. PDT efficiency was evaluated over this time by measuring the surface of the living spheroids, which was extracted from the picture with image J software as previously described [30]. Experiments were made in hexaplicate and three randomly selected pictures of each sample were analyzed. Unless specified, all data were expressed as mean ± SEM.

3. Results and discussion

Poly(ethyleneoxide-b-ε-caprolactone) (PEO-PCL, scheme 1) known to form various self-assemblies depending on the hydrophilic/hydrophobic balance is a routinely used copolymer for drug delivery vectors, owing to its well identified biocompatibility. Different molar masses of this polymer (table 1) were used (PEO-PCL 5000-11000, PEO-PCL 5000-4000, PEO-PCL 2000-7000, PEO-PCL 2000-4800), which produced nanovectors of various morphologies [11, 12].

Polymeric nano-objects were formed as previously described, using either a cosolvent approach where a polymer organic solution is added to pure water, or film rehydration followed by sonication/extrusion processes [11, 12]. They were characterized by transmission electron microscopy (TEM) and dynamic light scattering (DLS) (table 2). The morphology of each nano-structure was reported, showing that micelle-like, vesicular or worm-like self-assemblies were obtained. For PEO-PCL 2000-4800, our earlier studies have shown that self-assembly in water led to the formation of mixed morphologies (worm-like systems and vesicles), impeding a correct DLS analysis. The characterization of this system by AsFlFFF revealed the presence of three different populations of nano-objects centered around 80, 270 and 460 nm, which was also confirmed by TEM [12].

Controlled mixtures of nanovectors were obtained by mixing different ratios of these preformed nano-objects. As a typical case, mixtures of PEO-PCL 5000-4000 micelles/PEO-PCL 5000-11000 vesicles were obtained and thoroughly characterized by DLS or by AsFlFFF. DLS was performed using a custom-made program STORMS enabling fine adjustment of parameters to optimize fitting of the data (see supplementary information). DLS analysis is presented in figure 1 for different weight ratios of PEO-PCL 5000-11000.

PEO-PCL 5000-4000 micelles exhibited a size of 22 nm and the PEO-PCL 5000-11000 vesicles measured 88 nm. In these conditions, a micelle population of PEO-PCL 5000-4000 was detected but almost invisible as soon as PEO-PCL 5000-11000 content was higher than 20 wt%, when analyzed by intensity averages with the STORMS program. This is not surprising since the scattered intensity of an object is related to its size to the sixth [31], but this experiment is an unambiguous demonstration of this behavior.

When the same experiments were analyzed by the commercial Malvern software, the micelles were already invisible at 20 wt%. The advantage of the custom-made software STORMS is the possibility of modulating most parameters in

Table 3. DLS analysis of PEO PCL 5000 4000, PEO PCL 5000 11000 mixture at 80/20 wt/wt.

Alpha	Range	Expansion	Weighting[a]	PEO PCL 5000 4000 Int	PEO PCL 5000 11000 Int	80/20 mixture Int	PEO PCL 5000 4000 number	PEO PCL 5000 11000 number	80/20 mixture number
10	2	1	g	30	100	102	20	68	62
10	2	1	1	28	100	104	20	74	26
10	2	0	g	30	100	102	20	68	64
5	2	1	g	28	100	104	22	70	22
10	1	1	g	28	100	104/28	22	80	28
5	2	0	1	28	100	104	22	88	32
10	2	0	1	22	100	104	22	74	26
20	2	0	g	30	102	102	20	66	60
8	2	0	g	28	100	102	20	70	64
8	2	1	g	30	100	102	20	68	62

[a] 1 means that all points are used with the same weight, g that the weight of each point is linked to its value.

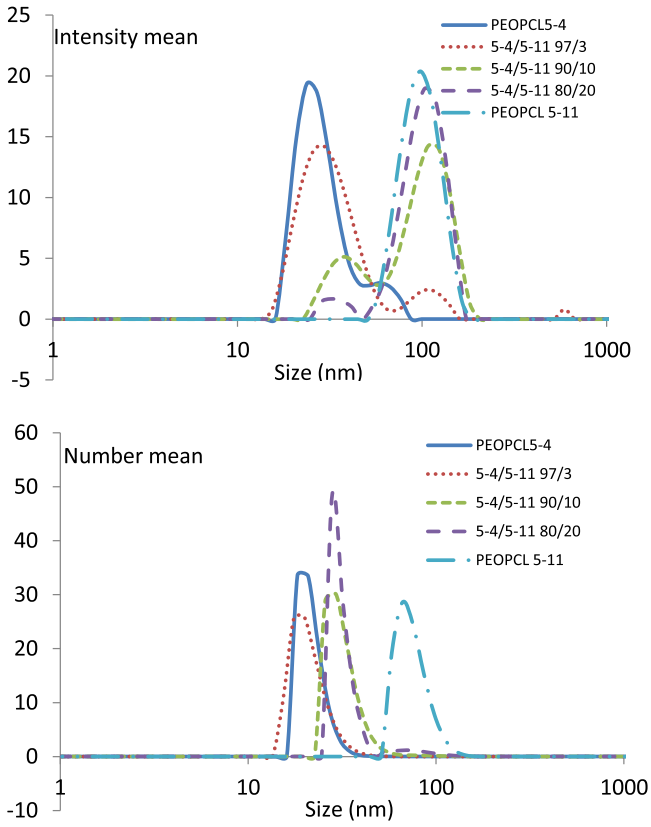

Figure 1. DLS analyses of PEO PCL 5000 4000 micelles (5 4)/PEO PCL 5000 11 000 vesicles (5 11) mixtures for different PEO PCL 5000 4000/PEO PCL 5000 11 000 weight ratios.

order to obtain perfect fitting of the correlograms, with residuals lower than 5×10^{-3}. A comparison of the results from Malvern and STORMS software is provided in supplementary information (figures S1-5 and tables S1-2). Interestingly, the number averaged analysis by STORMS did not show a double population but suggested a smooth increase of size with increasing ratio of PEO-PCL 5000-11000.

Thorough analysis was performed on the 80/20 wt% PEO-PCL 5000-4000 micelles/PEO-PCL 5000-11000 vesicles mixture to examine whether DLS analysis could show the presence of both populations, even in the number mean analysis. For this, several parameters were systematically changed in STORMS program: the regularization parameter (alpha), the distribution range, the expansion parameter (leading to the favored use of first points of the correlograms) and the weighting parameter (each point of the correlogram being addressed a different weight depending on its value). The results are presented in table 3. With the varying parameters, all intensity related results were stable. For number-relative analyses, the results obtained for pure micelles or vesicles were also stable, with a mean value of 21 ± 1 for micelles and 73 ± 7 for vesicles. For the 80/20 mixture, the situation was more complicated with a result clearly switching between ca. 22 32 and 60 64 nm depending on the fitting parameters. This unmistakably shows that DLS analysis cannot give unequivocal results even with a solution of controlled composition. Thus, unambiguous results cannot be expected using this approach for unknown solutions exhibiting several populations. In such system, the presence of a single population in DLS cannot be considered as a proof of the purity of the nano-objects. A similar example involving PEO-PCL 5000-11000 vesicles and PEO-PMMA 5000-11 900 micelles is presented in figures S4 and S5.

The same PEO-PCL 5000-4000 micelles/PEO-PCL 5000-11000 vesicles mixtures were then analyzed by AsFlFFF and the fractograms are shown in figure 2. This technique enabled the separation of both populations before their detection. Micelles were observed at an analysis time of ca. 14 min whereas vesicles eluted at ca. 26 min (figures 2(a) (d)). Thus, in this case, the ratio between micelles and vesicles can be directly observed from the refractive index signal. Zooming on MALLS signal fractogram between 11 and 17 min shows that quantities of micelles as low as 10 wt% were still observable without any doubt (figures 2(e) and (f)). Compared to the obtained DLS performance on the same sample, AsFlFFF allowed successfully separating and quantifying very dissimilar nano-objects in a single chromatographic injection.

In order to assess PDT efficiency, Pheo was loaded within PEO-PCL 5000-4000 micelles, PEO-PCL 5000-11000

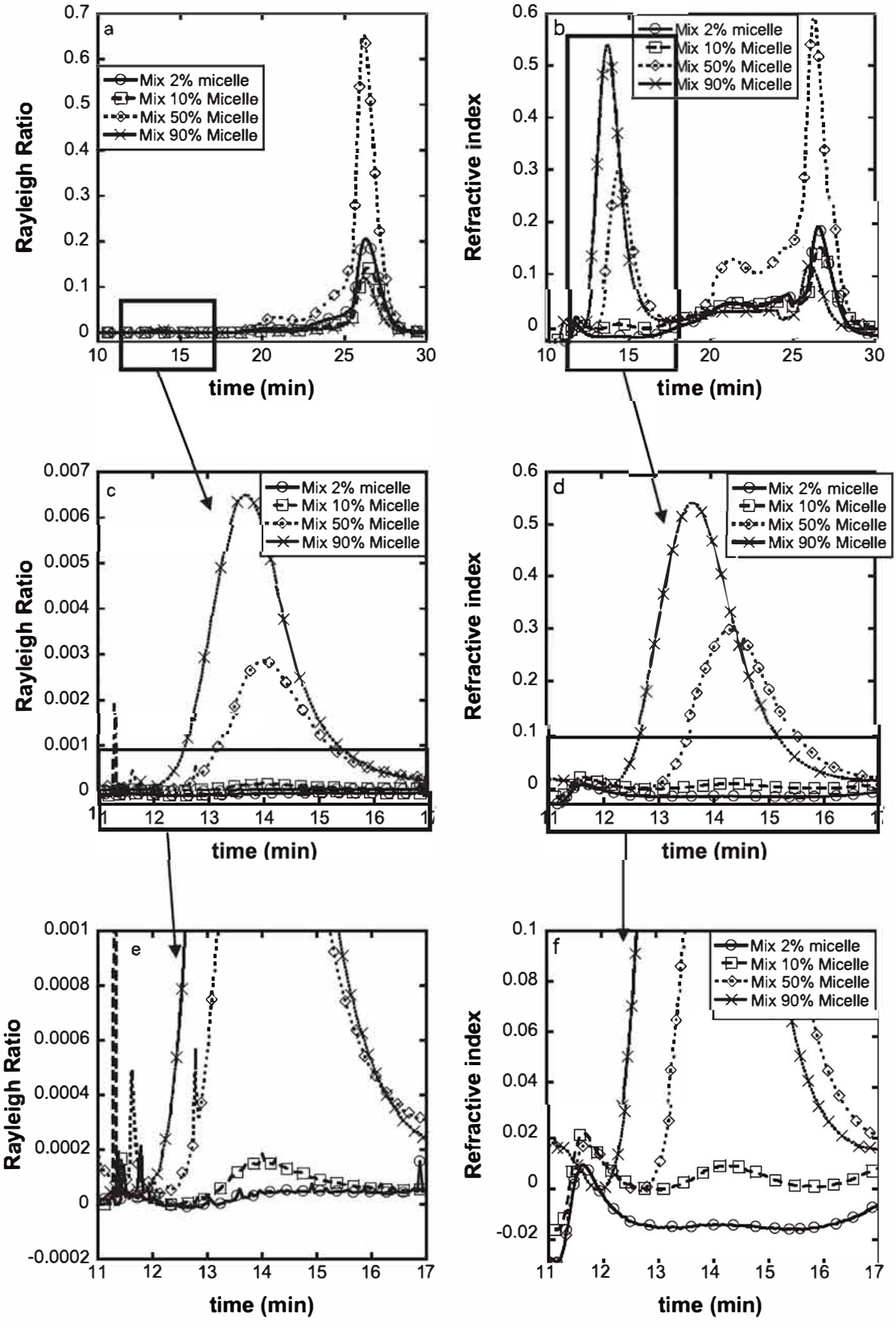

Figure 2. AsFlFFF fractogramms for PEO PCL 5000 4000/PEO PCL 5000 11000 mixtures. (a) MALLS signal; (b) RI signal; (c) and (e) MALLS signal, zoom of the micelle area; (d) and (f) RI signal, zoom of the micelle area. The indicated ratios are weight relative. o PEO PCL 5000 4000/PEO PCL 5000 11000 2/98 wt/wt; □ PEO PCL 5000 4000/PEO PCL 5000 11 000 10/90 wt/wt; ◊ PEO PCL 5000 4000/ PEO PCL 5000 11000 50/50 wt/wt; x PEO PCL 5000 4000/PEO PCL 5000 11000 90/10 wt/wt.

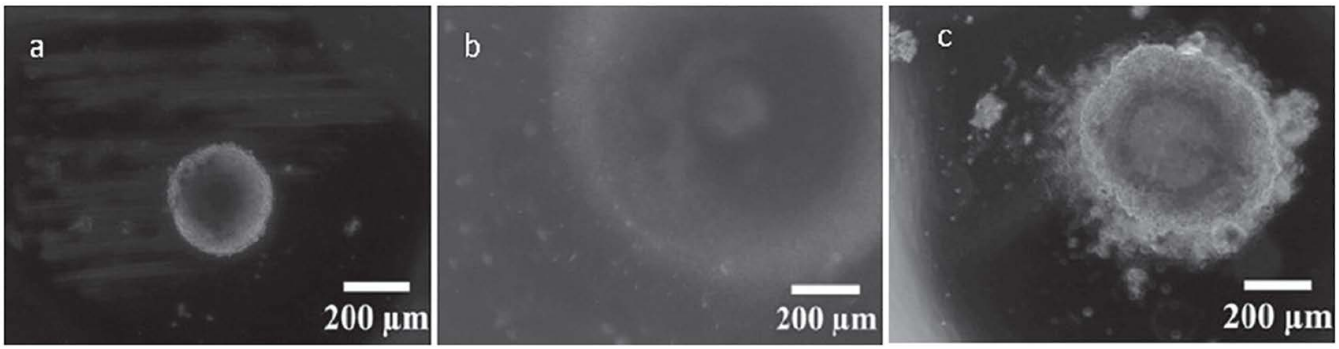

Figure 3. Typical wide field optical images of spheroids. (a) intact spheroid, (b) damaged FaDu spheroid (PEO PCL 2000 7000/PEO PCL 5000 11 000), (c) damaged HCT 116 spheroid (PEO PCL 5000 11000/PEO PCL 5000 4000).

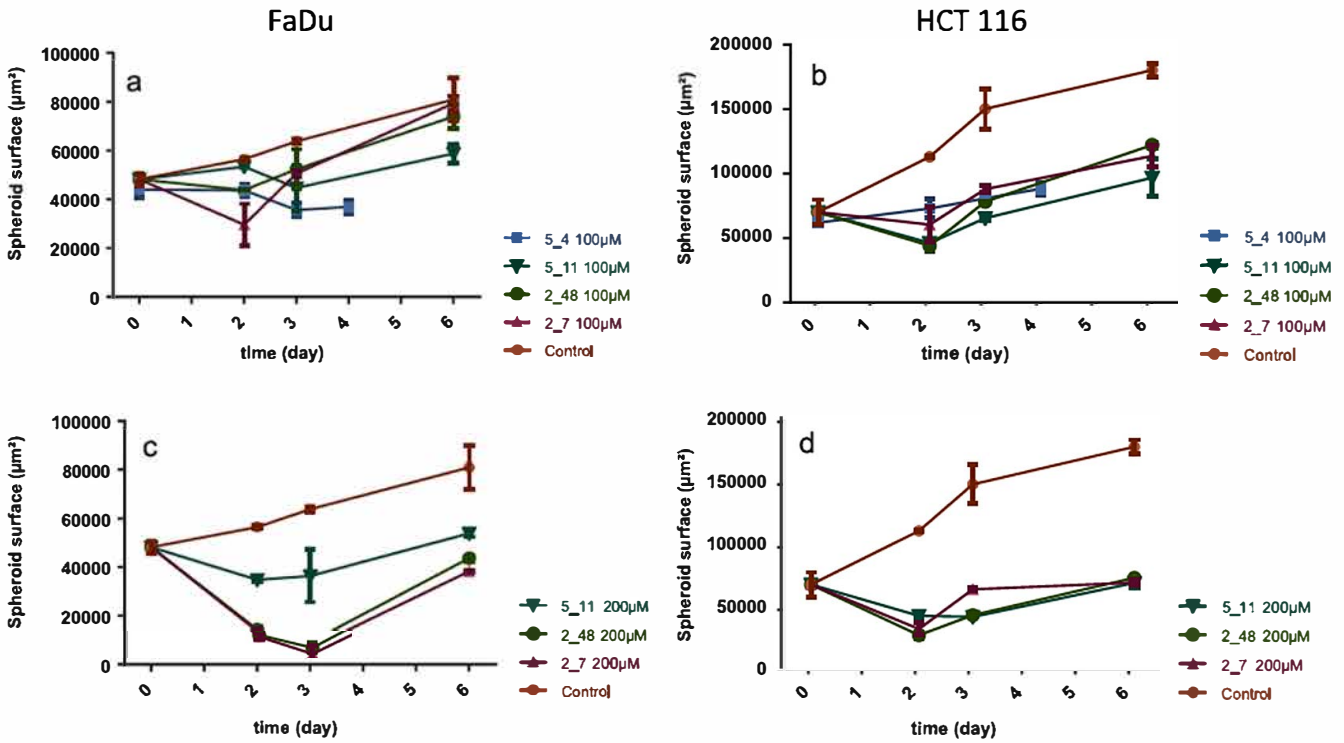

Figure 4. Spheroid size evolution upon PDT process. Left column, FaDu cells; right column, HCT 116 cells. Top line, [polymer] = 100 μM, [Pheo] = 3.33 μM. Bottom line, [polymer] = 200 μM, [Pheo] = 6.67 μM.

vesicles and PEO-PCL 2000-7000 worm-like systems. For this, the nano-objects were loaded directly during their formation for micelles or by post-addition for the vesicles formed by film rehydration/sonication/extrusion. It is noteworthy that for all systems described here our earlier studies on polymeric micelles have shown that the polymer/Pheo ratio can be adjusted so as to keep the size and morphology of the self-assemblies intact [10, 11, 32]. For this reason, this ratio in this work was kept at 30/1 mol/mol. For polymersomes, the influence of Pheo on the self-assemblies was checked by DLS (figure S6) and showed that these remained intact. Human spheroids of colon cancer (HCT-116) or head and neck cancer (FaDu) were formed, incubated with the Pheo-loaded nano-objects and irradiated to induce formation of reactive oxygen species leading to cell death [11]. PDT efficiency was evaluated by following the growth of the spheroids depending on the treatment. This was done by an optical method described in the experimental part and validated in an earlier study [30]. Typical images of spheroids are presented in figures 3 and S7, showing different cases of intact or damaged spheroids. Spheroid growths after PDT treatment are shown in figure 4 for single polymer nano-object solutions: PEO-PCL 5000-4000 micelles, PEO-PCL 5000-11000 vesicles, PEO-PCL 2000-4800 vesicular/worm-like system and PEO-PCL 2000-7000 worm-like nano-objects.

All vector types, regardless of their size or shape, led to an increase of PDT efficiency compared to non encapsulated Pheo (figure S8). Several points can be extracted from figure 4. First, compared to each other, all Pheo-loaded vectors exhibited similar activities, the only exception being the PEO-PCL 5000-11000 vesicles on FaDu cell line at 200 μM which were less

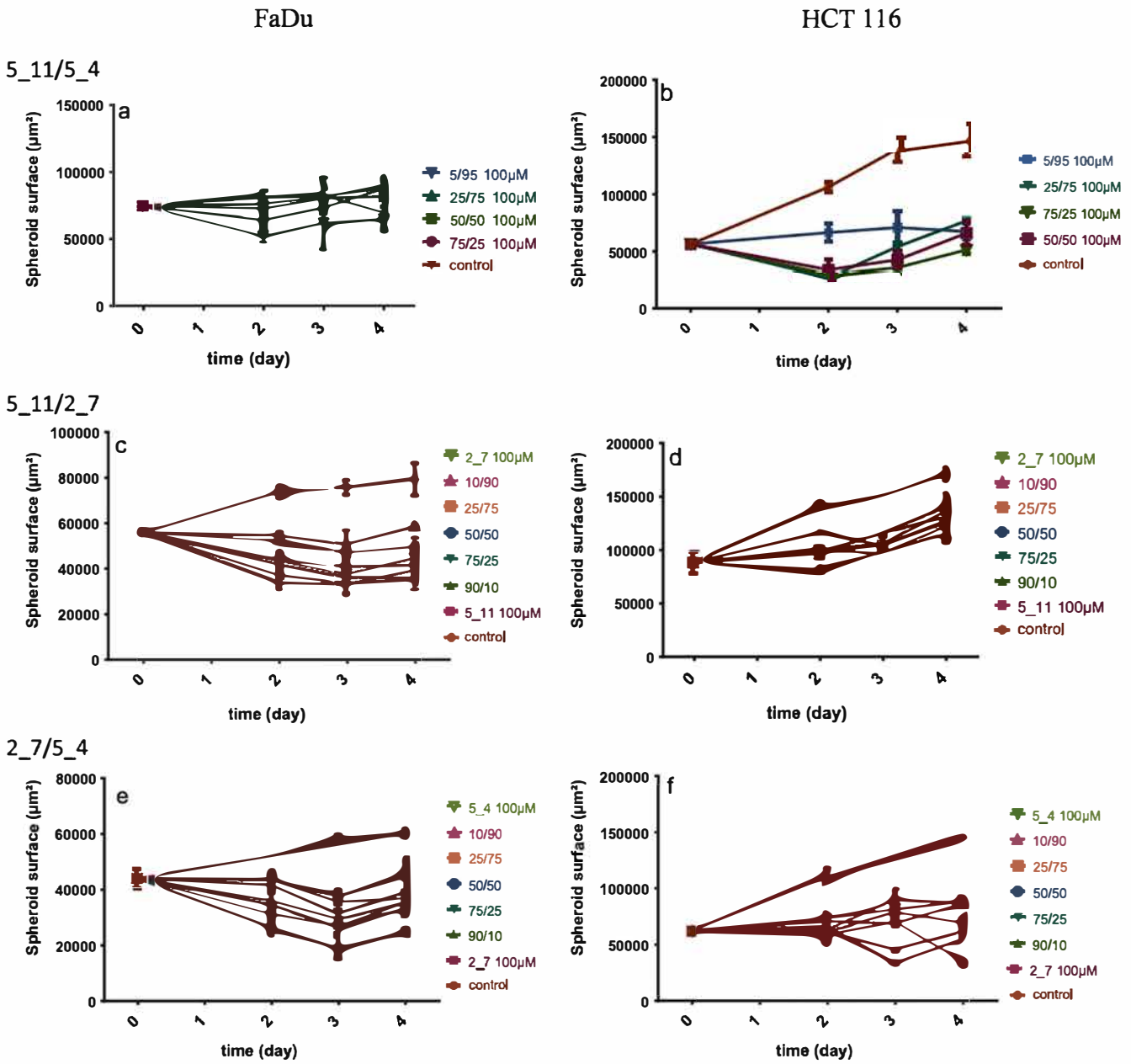

Figure 5. Spheroid size evolution upon PDT process. Left column, FaDu cells; right column, HCT 116 cells. (a) (b) PEO PCL 5000 11000 vesicles/PEO PCL 5000 4000 micelles mixtures. (c) (d) PEO PCL 5000 11000 vesicles/PEO PCL 2000 7000 worm like systems mixtures. (e) (f) PEO PCL 2000 7000 worm like systems/PEO PCL 5000 4000 micelles mixtures. The ratios are weight fractions.

efficient than the others in decreasing size of the tumor spheroids (figure 4(a)). PEO-PCL 2000-4800 nano-objects which consisted of mixed worm-like and vesicular systems also followed the general same trend, showing in this case an apparent absence of influence of the monomorphism of the vector solution.

Secondly, increasing Pheo concentration from 3.33 μM to 6.67 μM led to a better PDT efficiency. Indeed, the use of a Pheo concentration at 3.33 μM (figures 4(a) (b) provided an arrest in the spheroid growth whereas at 6.67 μM (figures 4(c) (d) a temporary decrease in size was observed.

Based on these preliminary results, we decided to use the lowest Pheo concentration of 3.33 μM for the subsequent experiments on mixtures (figure 5), in order to maximize the probability to discriminate efficiencies between pure solutions and controlled mixtures of preformed nano-objects.

Most curves of figure 5 show a clear difference between the control (spheroid without any polymer nor Pheo) and the Pheo-encapsulated nano-objects, leading to a decrease in the spheroid size or at least its stabilization. The only exception is the case of PEO-PCL 5000-11000/PEO-PCL 5000-4000 mixture on FaDu cells (figure 5(a)), for which only a small difference is visible between the control and the PDT treatment. Considering the experiments on FaDu cells, the mixtures incorporating PEO-PCL 2000-7000 worm-like systems (figures 5(c) and (e)) are the most efficient. This is however not

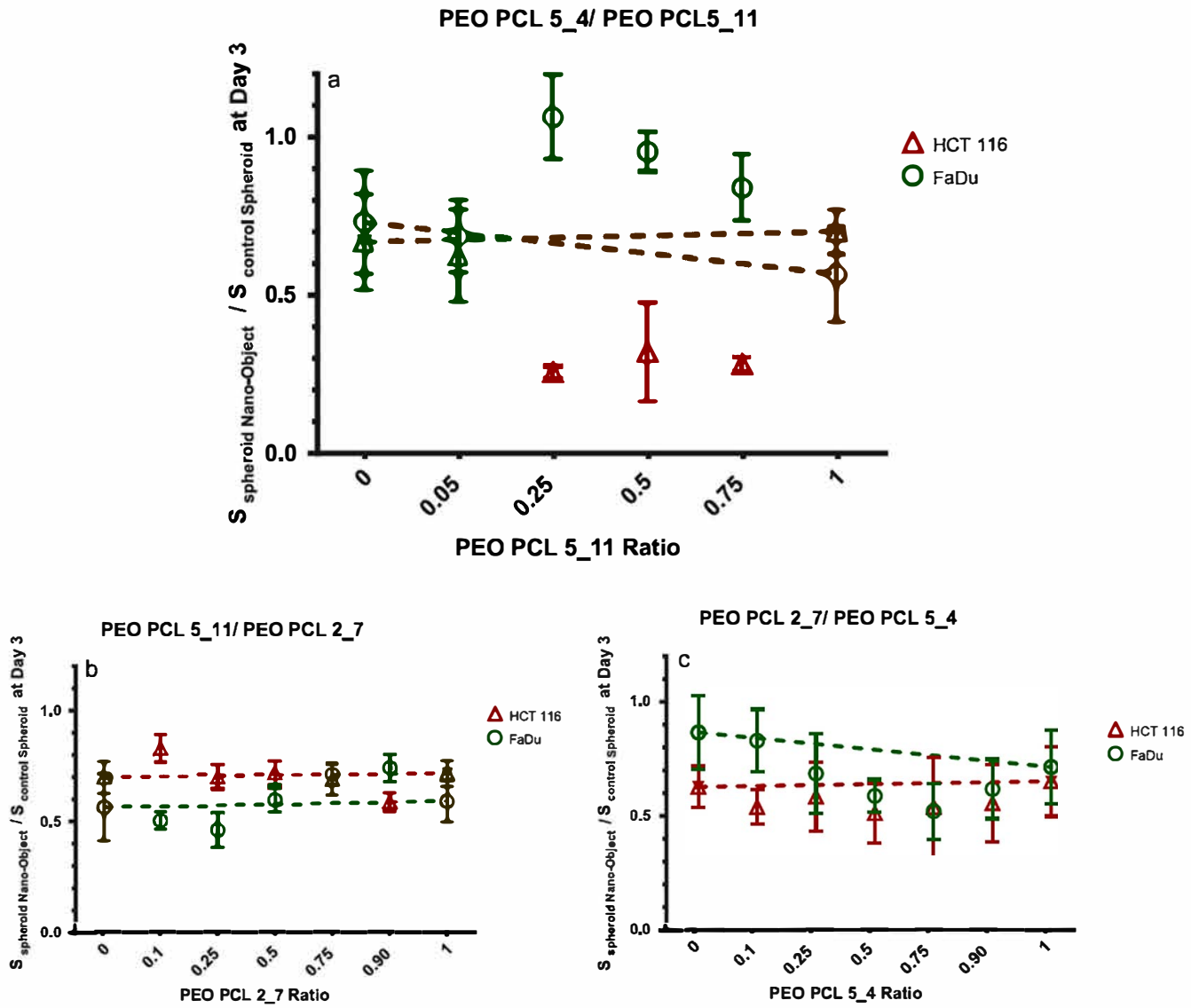

Figure 6. Compared spheroid size versus control at day 3 as a function of polymers ratio for the three different mixtures tested. Error bars are 95% confidence interval. Δ HCT 116 spheroids, o FaDu spheroids. (a) PEO PCL 5000 4000 micelles/PEO PCL 5000 11000 vesicles, (b) PEO PCL 5000 11000 vesicles/PEO PCL 2000 7000 worm like systems, (c) PEO PCL 2000 7000 worm like systems/PEO PCL 5000 4000 micelles.

true for the tests on HCT-116 cells where the micelles/vesicles mixture (figure 4(b)) has a similar activity to the others (figures 5(d) and (f)). It seems that nano-object purity does not affect distinct cell types similarly.

Comparing the experiments on FaDu cells to those on HCT-116 ones shows different situations. For vesicles/micelles mixtures (figures 5(a) and (b)), the PDT efficiency was higher on HCT-116 cells. This is consistent with the experiments on single polymer nanovectors (figures 4(a) and (b)) for this concentration of Pheo. For worm-like and vesicular systems (figures 5(c) and (d)), the reverse was observed. Finally, for micelles/worm-like systems mixtures (figures 5(e) and (f)), the PDT efficiency appeared close for both cell lines. These comments already show that the study of monomorphous nanovectors cannot lead to a prediction of the PDT efficiency of their mixture.

In order to better visualize mixture effects, the preceding results were analyzed at day 3, as a function of the ratio between polymers (figure 6). The parameter reported on these graphs is the ratio between the spheroid surfaces for the polymer mixture considered and the control. A curve with a down bell shape is therefore a sign of a mixture which is more efficient than either monomorphous nano-object; conversely, a curve with an upward bell shape shows that the mixture is less efficient. The dotted line is a guide showing the expected behavior if no synergy effect was present. On this figure, the error bars are 95% confidence intervals, ensuring that the conclusions drawn are valid.

Examining figure 6 shows that three different cases are present. First, the cases of PEO-PCL 2000-7000/PEO-PCL 5000-4000 on HCT-116 (figure 6(c)), PEO-PCL 5000-11000/ PEO-PCL 2000-7000 on either FaDu or HCT-116 cells (figure 6(b)) exhibited a change close to the theoretical one. In this case, the mixture is just a superimposition of the effect of both nano-objects, with neither increase nor decrease of the PDT

efficiency. The second case is that of PEO-PCL 5000-11000/PEO-PCL 5000-4000 on FaDu cells (figure 6(a)), showing that the mixture was less efficient than the theoretical dotted line. The explanation of this behavior is however not clear presently.

Finally, the most interesting cases were PEO-PCL 2000-7000/PEO-PCL 5000-4000 on FaDu cells (figure 6(c)) and PEO-PCL 5000-11000/PEO-PCL 5000-4000 on HCT-116 cells (figure 6(a)). For these, a synergy effect was observed, leading to a better PDT efficiency using the mixtures. For PEO-PCL 2000-7000/PEO-PCL 5000-4000 mixtures on FaDu cells, the best ratio was 25/75 w/w. In this case, the presence of both worm-like systems and micelles led to a better PDT efficiency. Interestingly, the mixture involving PEO-PCL 5000-4000 micelles and PEO-PCL 5000-11000 vesicles was observed to be more efficient in the case of HCT-116 spheroids (increase of 60% compared to the absence of synergy), contrary to that observed for FaDu (decrease of 60%).

To the best of our knowledge, no other study in the literature so far has examined the influence of the presence of different vector morphologies in the same experiment. However, the influence of size has been studied for a long time [4, 7, 33, 34] and that of shape is increasingly characterized. Indeed, several studies have suggested that worm-like nanovectors might be more efficient [13 15, 35 39]. Non-spherical nanovectors have been shown to have a longer circulation time, and the margination process mandatory for their exit from bloodstream has been shown to depend on the shape [37, 39 41]. Additionally, the cell penetration is also shape-sensitive, the worm-like systems exhibiting an increased penetration compared to spherical ones [38, 42]. In our hand, the worm-like PEO-PCL 2000-7000 micelles used as a monomorphous system were not observed to lead to a better therapeutic efficiency compared to spherical ones (either micelles or vesicles). The experiments presented here measured an overall PDT efficiency including several parameters, such as diffusion of the vector within the spheroid, penetration of the photosensitizer in the cell, generation of reactive oxygen species under irradiation, and cell death induction. In order to fully examine the influence of the shape for PDT vectors, a further complete study would be necessary to determine the mechanisms of cell penetration. Indeed, in such systems, the photosensitizer cell penetration could be either in its encapsulated or free form [43, 44]. However, the fact that mixtures exhibited either neutral, synergistic or antagonistic behaviors shows that the vectors are not eliminated at the surface of the spheroids.

4. Conclusion

The objective of this work was to characterize mixtures of polymeric vectors and examine the influence of their purity in photodynamic therapy efficiency on *in vitro* 3D tumor models. For this purpose, we produced and characterized different PEO-PCL nanovectors with micellar, vesicular and worm-like morphologies. We clearly demonstrated that batch DLS should not be used in the presence of mixtures and that AsFlFFlF was the most adapted and efficient method to characterize the polymorphism of nano-object solutions. When assessed *in vitro* in PDT tests, some controlled mixtures of micelles, vesicles or worm-like structures exhibited a synergistic effect compared to monomorphous nanovectors. At this point, only assumptions can be made that the presence of both types of morphologies may improve the diffusion process. Further work will be necessary to confirm this hypothesis.

Acknowledgments

This work was funded by the French ANR P2N COPOPDT, Midi-Pyrénées region and University of Toulouse.

Supporting information

Details on DLS analyses, development and use of STORMS software, other examples of nano-object mixtures, typical wide-field optical images of HCT-116 and FaDu spheroids, effect of unencapsulated Pheo on spheroids.

References

[1] Matsumura Y and Maeda H 1986 *Cancer Res.* **46** 6387 92
[2] Riehemann K, Schneider S W, Luger T A, Godin B, Ferrari M and Fuchs H 2009 *Angew. Chem. Int. Ed.* **48** 872 97
[3] Shi J, Votruba A R, Farokhzad O C and Langer R 2010 *Nano Lett.* **10** 3223 30
[4] Bertrand N and Leroux J C 2012 *J. Control. Release* **161** 152 63
[5] Lee J S and Feijen J 2012 *J. Control. Release* **161** 473 83
[6] Krasia Christoforou T and Georgiou T K 2013 *J. Mater. Chem.* B **1** 3002 25
[7] Messager L, Gaitzsch J, Chierico L and Battaglia G 2014 *Curr. Opin. Pharmacol.* **18** 104 11
[8] Habel J *et al* 2015 *RSC Adv.* **5** 79924 46
[9] Knop K, Mingotaud A F, El Akra N, Violleau F and Souchard J P 2009 *Photochem. Photobiol. Sci.* **8** 396 404
[10] Ehrhart J, Mingotaud A F and Violleau F 2011 *J. Chromatogr.* A **1218** 4249 56
[11] Gibot L *et al* 2014 *Biomacromolecules* **15** 1443 55
[12] Till U, Gaucher Delmas M, Saint Aguet P, Hamon G, Marty J D, Chassenieux C, Payré B, Goudounèche D, Mingotaud A F and Violleau F 2014 *Anal. Bioanal. Chem.* **406** 7841 53
[13] Liu Y, Tan J, Thomas A, Ou Yang D and Muzykantov V R 2012 *Ther. Delivery* **3** 181 94
[14] Fish M B, Thompson A J, Fromen C A and Eniola Adefeso O 2015 *Ind. Eng. Chem. Res.* **54** 4043 59
[15] Williford J M, Santos J L, Shyam R and Mao H Q 2015 *Biomater. Sci.* **3** 894 907
[16] Master A, Livingston M and Sen Gupta A 2013 *J. Control. Release* **168** 88 102
[17] Brown S B, Brown E A and Walker I 2004 *Lancet Oncology* **5** 497 508
[18] Miller J W *et al* 1999 *Arch. Ophtalmol.* **117** 1161 73
[19] Jang W D *et al* 2005 *Angew. Chem., Int. Ed. Engl.* **44** 419 23
[20] Nishiyama N, Morimoto Y, Jang W D and Kataoka K 2009 *Adv. Drug Deliv. Rev.* **61** 327 38

[21] Shibu E S, Hamada M, Murase N and Biju V 2013 *J. Photochem. Photobiol.* C **15** 53 72
[22] Li B, Moriyama E H, Li F, Jarvi M T, Allen C and Wilson B C 2007 *Photochem. Photobiol.* **83** 1505 12
[23] Derycke A S and de Witte P A 2004 *Adv. Drug Deliv. Rev.* **56** 17 30
[24] Couleaud P, Morosini V, Frochot C, Richeter S, Raehm L and Durand J O 2010 *Nanoscale* **2** 1083 95
[25] Kuntsche J, Freisleben I, Steiniger F and Fahr A 2010 *Eur. J. Pharm. Sci.* **40** 305 15
[26] Taillefer J, Brasseur N, van Lier J E, Lenaerts V, Garrec D L and Leroux J C 2001 *J. Pharm. Pharmacol.* **53** 155 66
[27] Le Garrec D, Taillefer J, Van Lier J E, Lenaerts V and Leroux J C 2002 *J. Drug Targeting* **10** 429 37
[28] Gibot L and Rols M P 2013 *J. Membrane Biol.* **246** 745 50
[29] Gibot L, Wasungu L, Teissie J and Rols M P 2013 *J. Control. Release* **167** 138 47
[30] Till U, Gibot L, Vicendo P, Rols M P, Gaucher G, Violleau F and Mingotaud A F 2016 *RSC Adv.* submitted
[31] Dionzou M *et al* 2016 *Soft Matter* **12** 2166 76
[32] Knop K, Mingotaud A F, El Akra N, Violleau F and Souchard J P 2009 *Photochem. Photobiol. Sci.* **8** 396 404
[33] Meng F and Zhong Z 2011 *J. Phys. Chem. Letters* **2** 1533 9
[34] Deng C, Jiang Y, Cheng R, Meng F and Zhong Z 2012 *Nano Today* **7** 467 80
[35] Cai S, Vijayan K, Cheng D, Lima E M and Discher D 2007 *Pharm. Res.* **24** 2099 109
[36] Cabral H and Kataoka K 2010 *Sci. Technol. Adv. Mater.* **11** 014109
[37] Toy R, Hayden E, Shoup C, Baskaran H and Karathanasis E 2011 *Nanotechnology* **22** 115101
[38] Vacha R, Martinez Veracoechea F J and Frenkel D 2011 *Nano Lett.* **11** 5391 5
[39] Vahidkhah K and Bagchi P 2015 *Soft Matter* **11** 2097 109
[40] Gentile F, Chiappini C, Fine D, Bhavane R C, Peluccio M S, Cheng M M C, Liu X, Ferrari M and Decuzzi P 2008 *J. Biomech.* **41** 2312 8
[41] D'Apolito R *et al* 2015 *J. Control. Release* **217** 263 72
[42] Yue T, Xu Y, Sun M, Zhang X and Huang F 2016 *Phys. Chem. Chem. Phys.* **18** 1082 91
[43] Kerdous R, Sureau F, Bour A and Bonneau S 2015 *Int. J. Pharm.* **495** 750 60
[44] Xu P, Gullotti E, Tong L, Highley C B, Errabelli D R, Hasan T, Cheng J X, Kohane D S and Yeo Y 2009 *Mol. Pharm.* **6** 190 201

Supplementary information for

Self-assembled polymeric vectors mixtures: characterization of the polymorphism and existence of synergetic effects in photodynamic therapy

Ugo Till [a,b], Laure Gibot[c], Christophe Mingotaud[b], Patricia Vicendo[b], Marie-Pierre Rols[c], Mireille Gaucher[a], Frédéric Violleau[d*] and Anne-Françoise Mingotaud [b*]

I. Characteristics of other polymer self- assemblies used

Polymer	Mn of PEO block ($g.mol^{-1}$)	Mn of hydrophobic block ($g.mol^{-1}$)	$f_{hydrophilic}$ [a] (%)	Preparation method
PEOPMMA 5000-11900	5000	11900	29.6	Acetone cosolvent

[a] weight fraction of hydrophilic part

Polymer	D_H (nm) intensity average	D_H (nm) Number average	PDI	Morphology
PEOPMMA 5000-11900	35	25	0.22	micelles

II. Development and use of STORMS software

The Malvern software is very efficient to acquire experimental data and to analyze them in a predefined way. However, changing the parameters of such an analysis and comparing various models are not so easy even if one can modify in a step-by-step and repeating way the details of each data treatment. Furthermore, the Malvern software is often just a black box: very little information is available concerning the various calculations and assumptions made for an analysis.

STORMS program is a software purely designed for the analysis of data and offering an easy choice in the methods used to extract information from the correlograms, to evaluate the distributions in intensity then in number. Implementation of different models describing non spherical particles, of mathematical treatment of correlograms, of scattering properties models have been made to test various possibilities and adjust the analysis depending on the type of samples. Pre-selected parameters were chosen in order to describe easily micelles and vesicles made of organic compounds such as surfactants or polymers, or mixtures of them. Finally, a routine of this software calculates the theoretical correlogram of a solution containing various particles. This may then be analyzed and compared to experimental data.

Figure S1 presents a screen copy showing the overall presentation of the software with the different parameters that can be changed. The program uses exported correlograms from Malvern. The fitting method can be adjusted, together with the regularization parameter (alpha), the distribution range, the expansion parameter (leading to the favored use of first points of the correlograms) and the weighting parameter. The geometry of the particle can also be adapted from spheres, ellipsoid, nano-rods or worm-like systems. Finally, the morphology of the scattering object can be chosen between full spheres, coated spheres, vesicles or mixtures.

In the right part of the window, the correlogram is shown together with the fitting (red curve), followed by the residual, the intensity relative analysis and the number relative one.

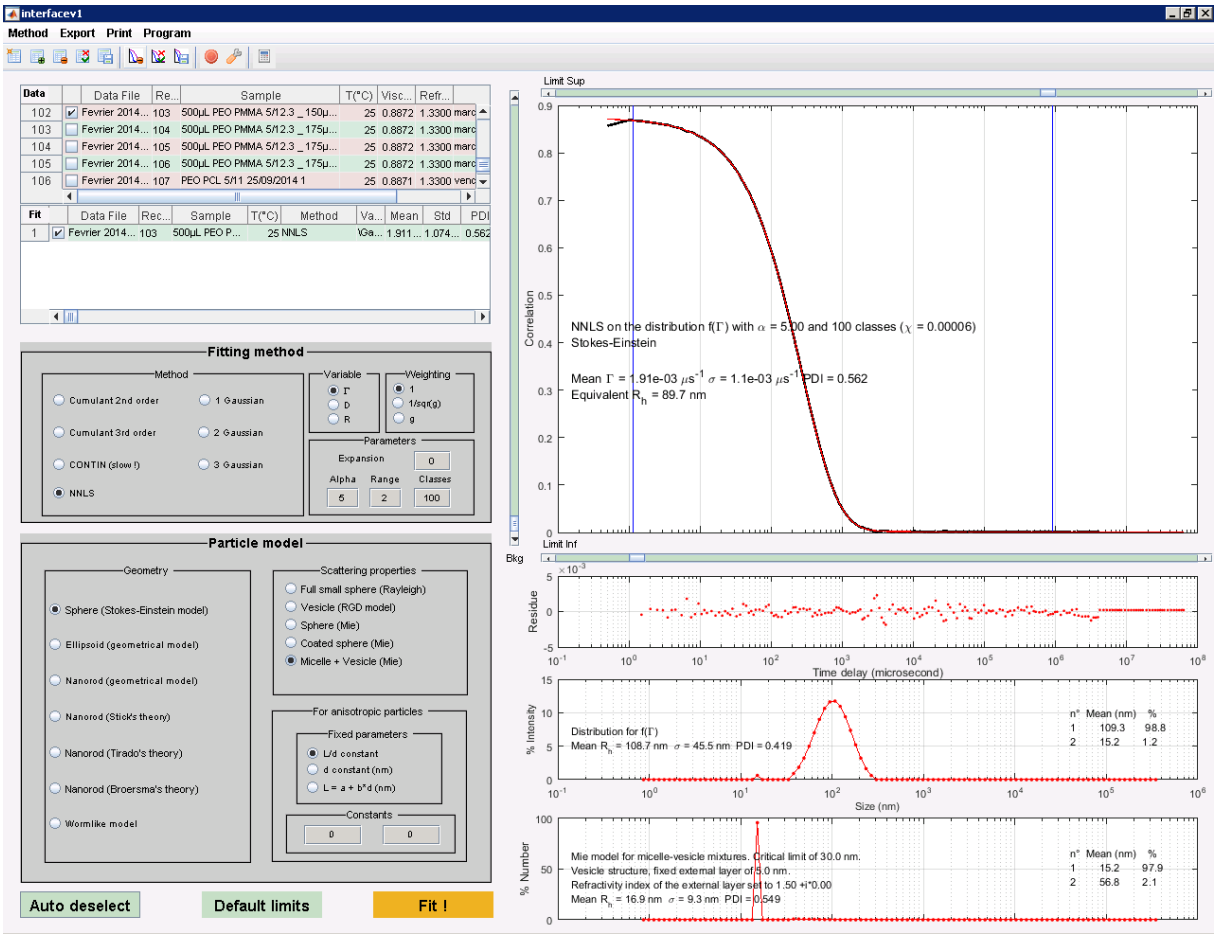

Fig S1. STORMS software presentation

In a more precise way, STORMS has been written and compiled with MATLAB (version R2015b).

The Cumulant method was based on the paper of B.J Frisken (Frisken, B. J. (2001). Revisiting the method of cumulants for the analysis of dynamic light-scattering data. *Appl. Opt.*, 4087-91) with the fitting of the autocorrelation function using the equation:

$$g^{(2)}(\tau) = B + \beta.e^{-2.\bar{\Gamma}.\tau}.\left(1 + \frac{\mu_2}{2!}.\tau^2 - \frac{\mu_3}{3!}.\tau^3 + \cdots\right)^2$$

where B is the background value, β the amplitude of the autocorrelation function, $\bar{\Gamma}$ the mean value of the decay rates and μ_n the n^{th} moment of the distribution function of decay rates, $f(\Gamma)$. The moments about the mean are defined as:

$$\mu_n = \int_0^\infty f(\Gamma).(\Gamma - \bar{\Gamma})^n \, d\Gamma$$

and are related to the cumulants.

This analysis leads to the so-called PDI (polydispersity index) is defined as the ratio between the second moment of the distribution divided by the square of the mean value of the decay rate. Generally speaking, the estimated PDI in STORMS is much larger than the one calculated by the MALVERN software since all the experimental points are selected and the second order equation is used in STORMS instead of the third one for Malvern.

Non-Negatively constrained Least Squares (NNLS) algorithm is using a regularization process, called the second-order Tikhonov regularizor. The importance of the regularization is modified by a parameter λ, which is estimated through the minimization of a Lagrange function (see Hansen, P. C. (2008). Regularization Tools. A Matlab Package for Analysis and Solution of Discrete Ill-Posed Problems. www.mathworks.com/matlabcentral/filiexchange and *Numer. Algor.* **46** (2007) 189-94.).

The CONTIN method, originally developed by S. W. Provencher (Provencher, S. W. (1984) http://s-provencher.com/pages/contin.shtml and *Comput. Phys. Com.* **27** (1982) 229-42.) was included in STORMS through a routine largely using codes written by I.-G. Marino and available on the web (http://www.mathworks.com/matlabcentral/fileexchange/6523-rilt).

For the calculation of the Mie model, a routine based on the program written by J. Schäfer (http://www.mathworks.com/matlabcentral/fileexchange/36831-matscat) was developed.

STORMS allows one to select and weight the experimental points of each correlogram. In the current paper, all these points were kept and had the same weight (except in the tests of table 2).

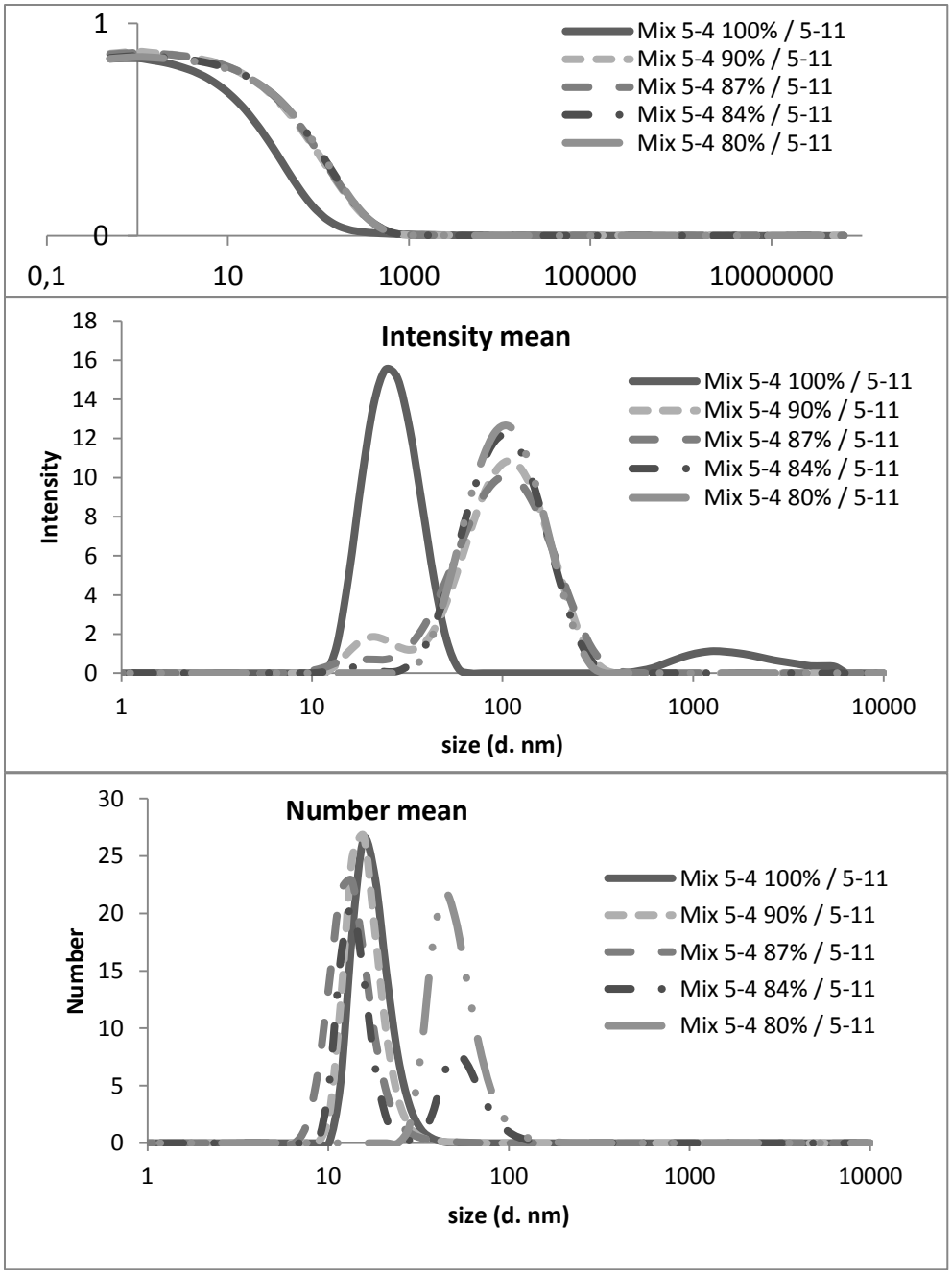

Figure S2. DLS analysis of PEO-PCL 5000-4000 / PEO-PCL 5000-11000 mixtures. Analysis by Malvern

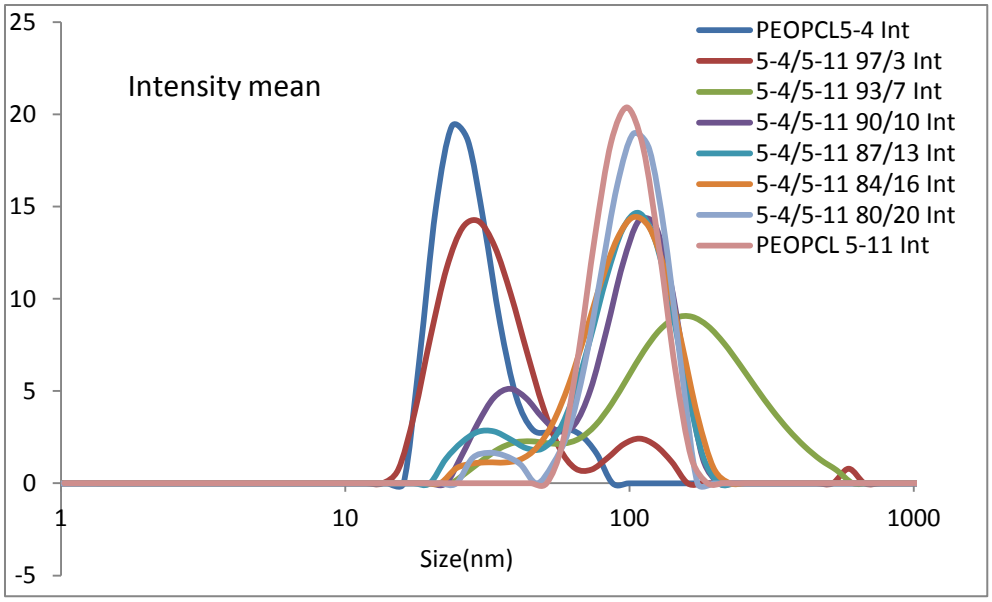

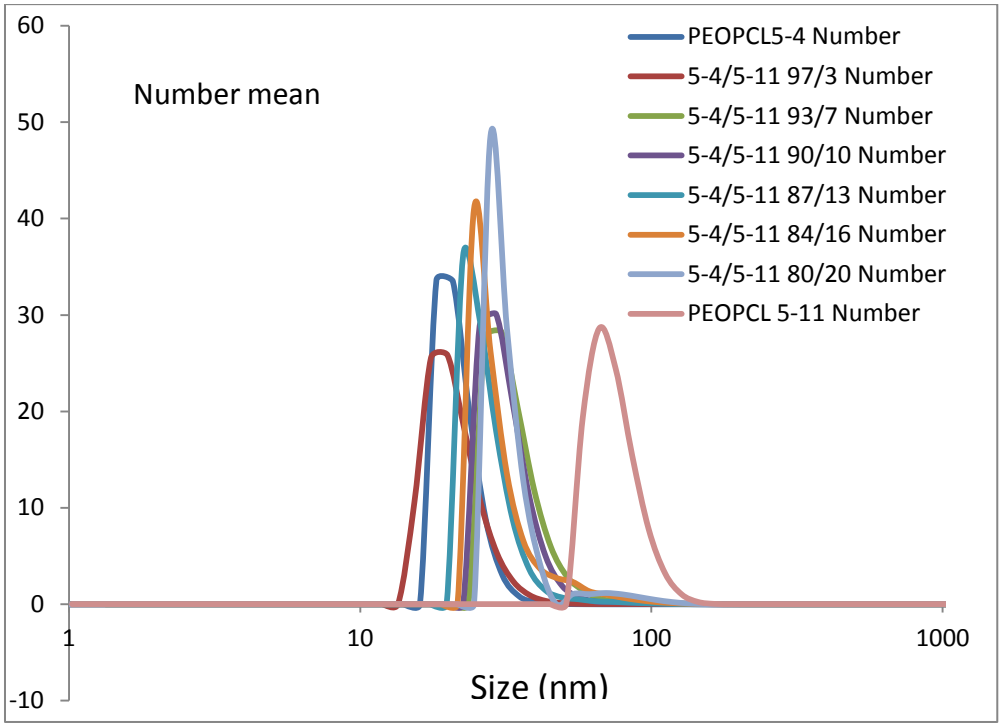

Figure S3. DLS of PEOPCL 5-4 / PEOPCL 5-11 systems, analysis by STORMS.

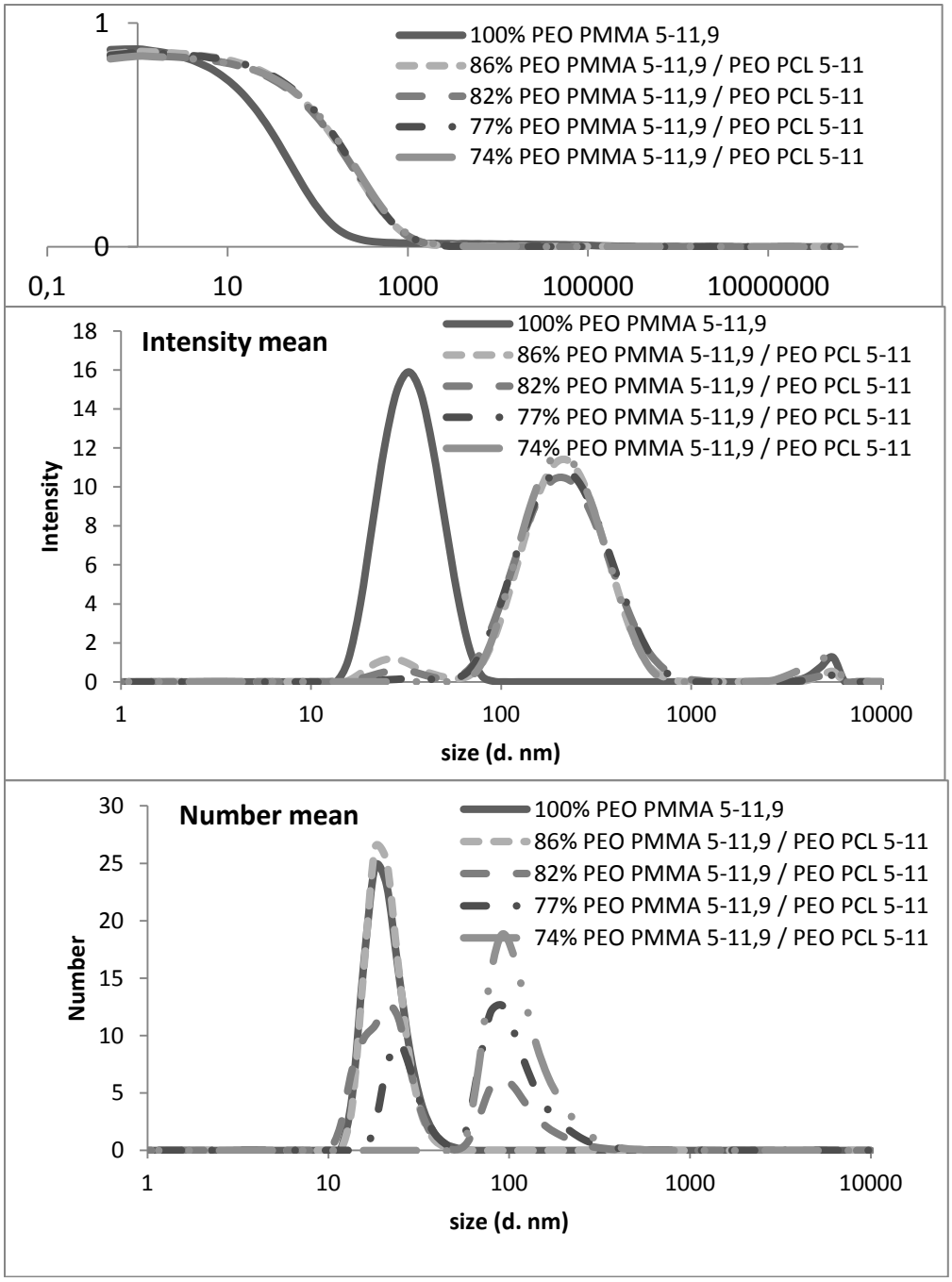

Figure S4. DLS analysis of PEO-PMMA 5000-11900 / PEO-PCL 5000-11000 mixtures. Analysis by Malvern program

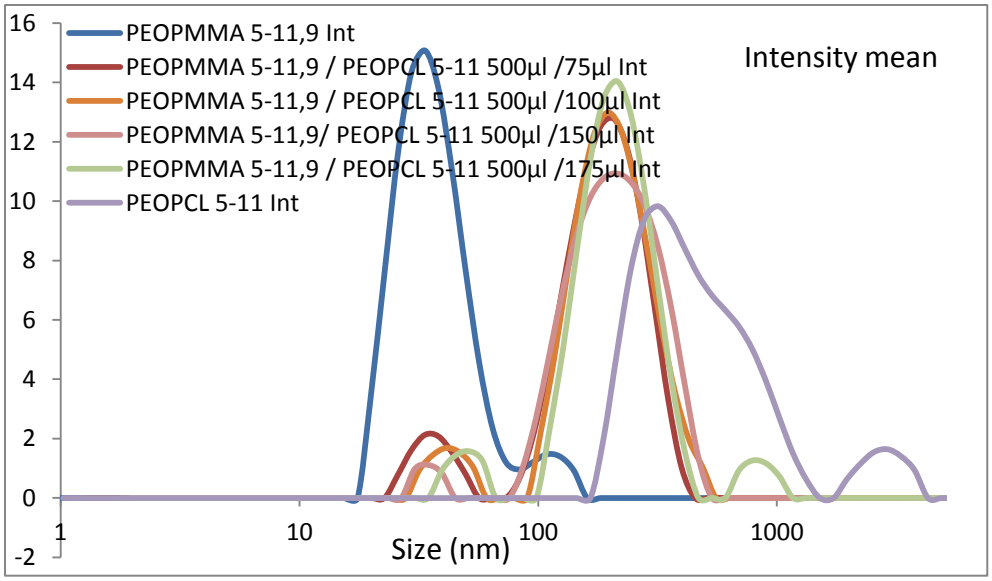

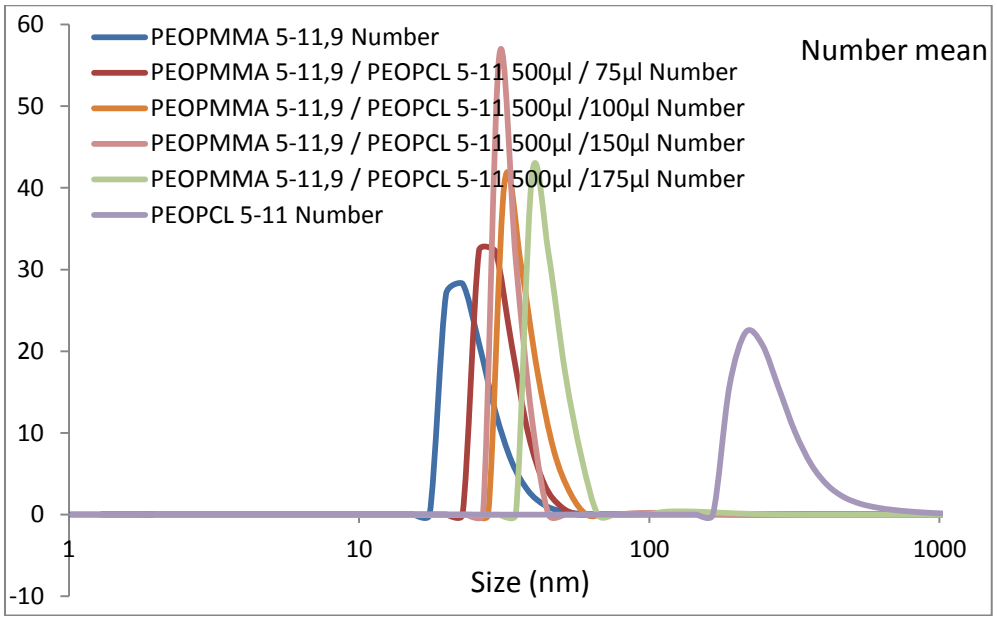

Figure S5. DLS analysis of PEO-PMMA 5000-11900 / PEO-PCL 5000-11000 mixtures. Analysis by STORMS

For this synthesis of PEO-PCL 5000-11000 vesicles, the size obtained was larger than the usual one (see main text and tables S1 and S2). This can happen if the dried film used before rehydration is not regular and too thick. For the purpose of this physical chemistry study however, this was not problematic and we proceeded to the study of the mixtures.

The corresponding data are provided in tables S1 and S2 for these two systems.

	STORMS							MALVERN			
Mixture	diam int	% int	PDI int	diam number	% number	PDI number		diam int	% Int	PDI	diam number
PEO PCL 5/4	27.6	89	0.4	21.6		0.17		27		0.26	17.7
	60	11									
PEO PCL 5/4 97/3 PEO PCL 5/11	32	88	1.3	21		0.23		28	80	0.33	17.8
	104	10						468	20		
PEO PCL 5/4 93/7 PEO PCL 5/11	182	89	0.6	34		0.3		212	87	0.43	23.7
	42	11						34	11		
PEO PCL 5/4 90/10 PEO PCL 5/11	110	74	0.42	32		0.25		116	91	0.28	16.6
	52	26						23	9		
PEO PCL 5/4 87/13 PEO PCL 5/11	103.6	86	0.39	28		0.28		109		0.26	15.5
	33.6	14									
PEO PCL 5/4 84/16 PEO PCL 5/11	100		0.35	31.2		0.37		115	98	0.22	14.3
								17	2		
PEO PCL 5/4 80/20 PEO PCL 5/11	104	94	0.28	31	94	0.32		112		0.18	53
	34	6		76	6						
PEO PCL 5/11	99.6		0.23	88		0.25		106		0.1	60

Table S1. Comparison of DLS results from STORMS and Malvern softwares for PEO-PCL 5000-4000 / PEO-PCL 5000-11000 mixtures.

	STORMS							MALVERN			
mixture	diam int	% int	PDI int	diam number	% number	PDI number		diam int	% int	PDI	diam number
PEO PMMA 5/11.9	36	93	8.9	25		0.22		35.5		0.26	20
PEO PMMA 5/11.9 86/14 PEO PCL 5/11	218	91	0.43	33		0.26		221		0.3	20.2
	40	9									
PEO PMMA 5/11.9 82/18 PEO PCL 5/11	218	93	0.43	36		0.3		222		0.3	116
	42	7									
PEO PMMA 5/11.9 77/23 PEO PCL 5/11	224		0.42	32		0.33		248		0.27	112
PMMA 5/11.9 74/26 PEO PCL 5/11	220	91	0.62	44	98	0.37		232		0.34	119
	50	5									
PEOPCL 5-11	576		11.8	276		0.44		475		0.39	145

Table S2. Comparison of DLS results from STORMS and Malvern softwares for PEO-PMMA 5000-11900 / PEO-PCL 5000-11000 mixtures.

For both mixture families, the intensity relative results estimated by the two softwares are similar. Small variations are sometimes observed for a second population. For the number relative analysis, the behavior is more complex and different results are sometimes obtained, owing to the possible different scattering properties concerned. Indeed, Malvern software always considers the Mie scattering theory for spherical filled objects. In STORMS, the option considering a mixture of micelles (for the object below 25 nm of radius) and vesicles was chosen.

Figure S6. Batch DLS analyses of PEO-PCL 5000-11000 and PEO-PCL 2000-7000 polymersomes in the absence and the presence of Pheo ([polymer] / [Pheo] = 30)

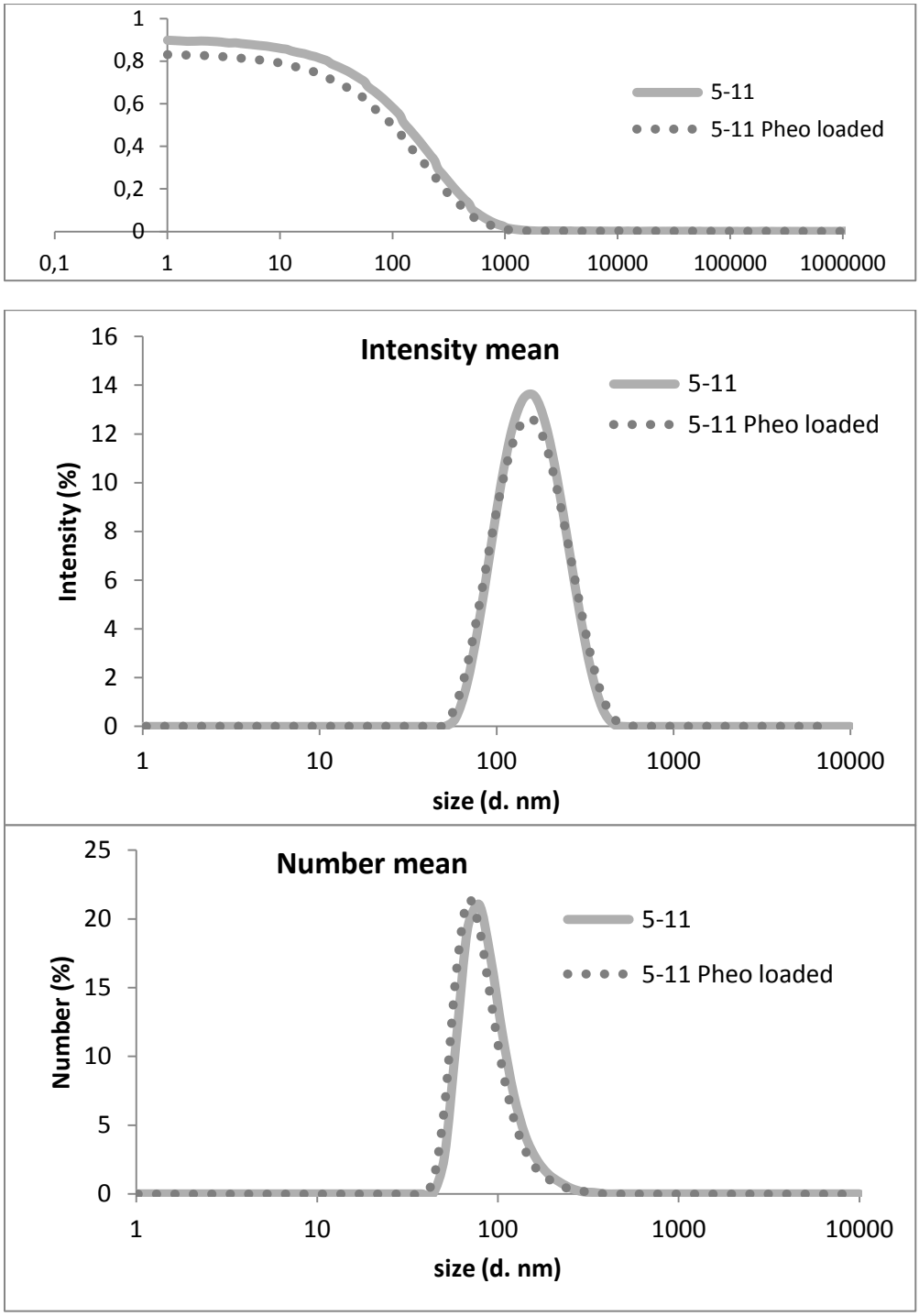

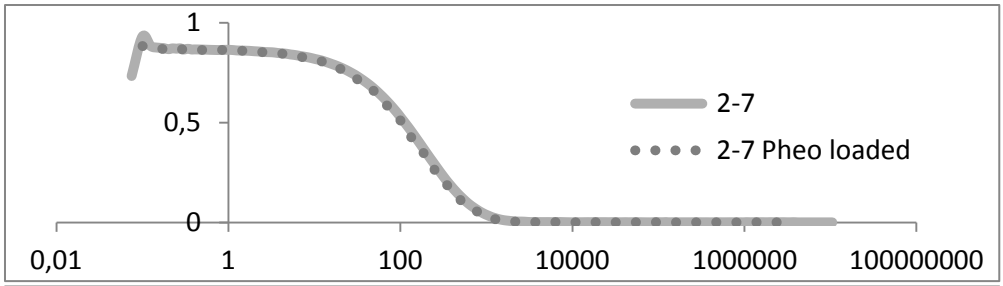
1
0,5
0
0,01
1
100
10000
1000000
100000000
2-7
2-7 Pheo loaded

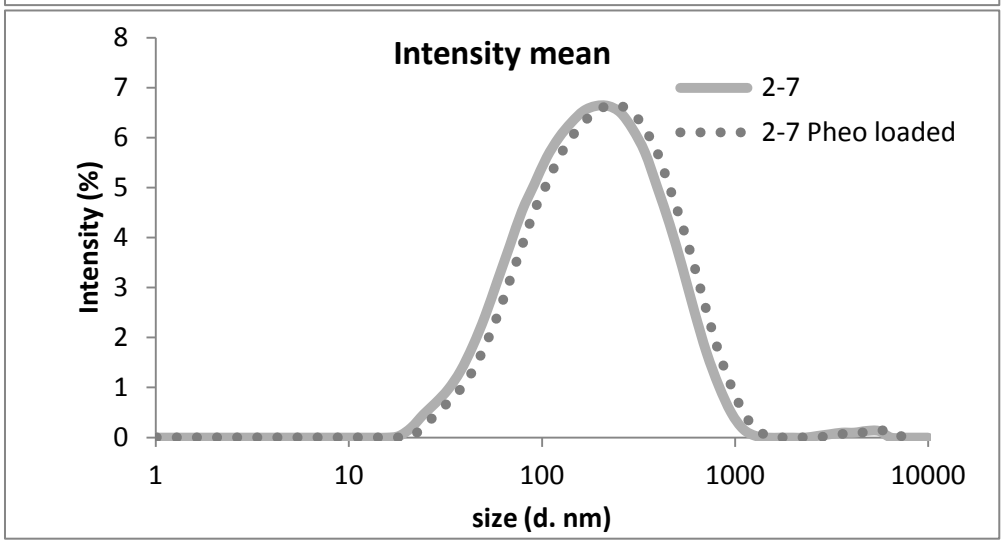
Intensity mean
Intensity (%)
8
7
6
5
4
3
2
1
0
1
10
100
1000
10000
size (d. nm)
2-7
2-7 Pheo loaded

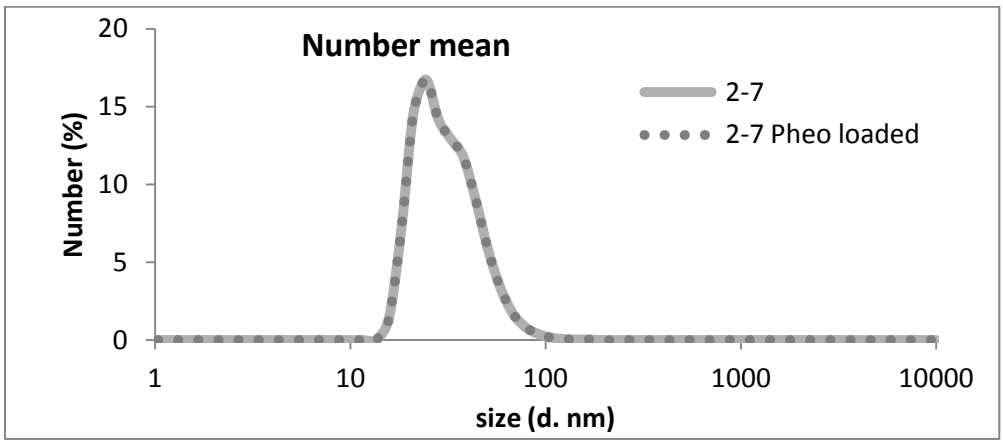
Number mean
Number (%)
20
15
10
5
0
1
10
100
1000
10000
size (d. nm)
2-7
2-7 Pheo loaded

Figure S7: Typical wide-field optical images of HCT 116 and FaDu spheroids following different treatments.

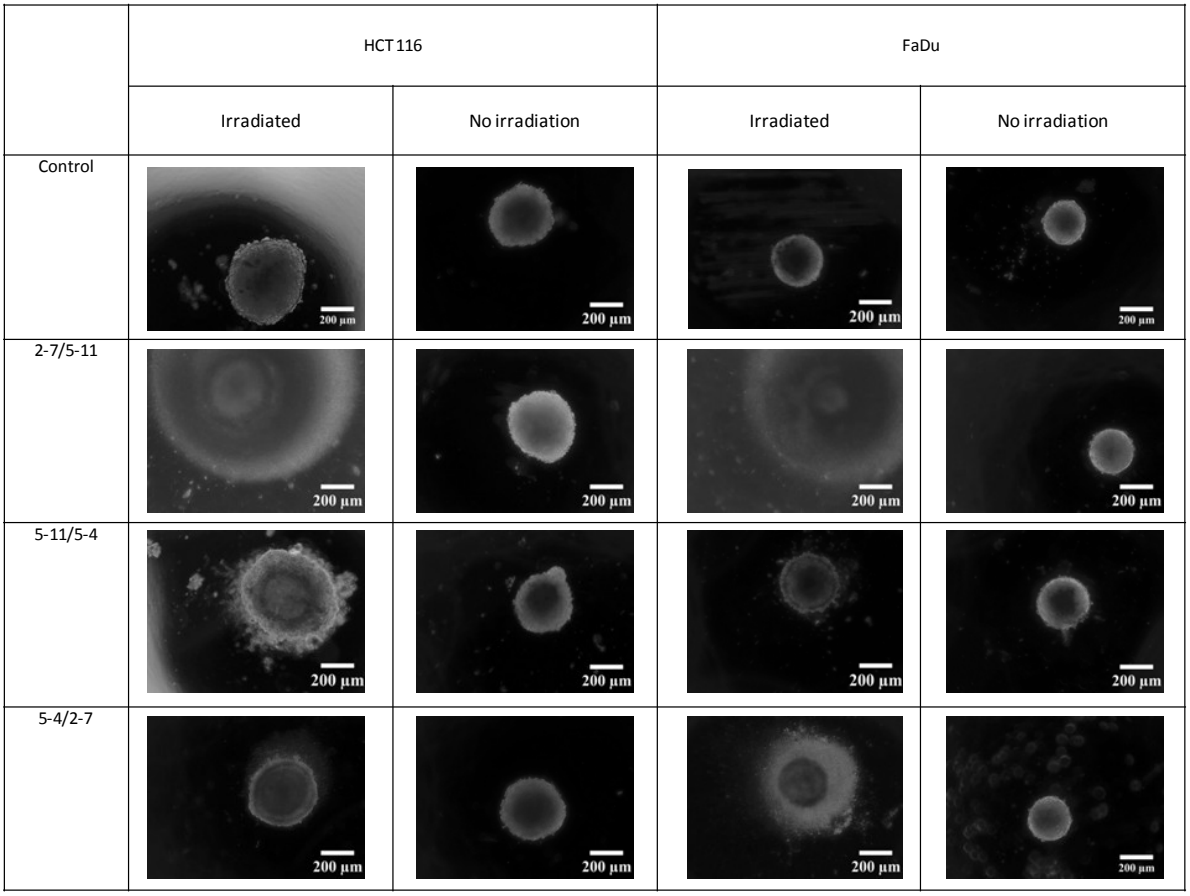

Figure S8: Effect of unencapsulated Pheo on spheroids ($[Pheo]_0$ = 3.3 µM)." Control" describes spheroids alone, without any polymer nor Pheophorbide, which is submitted to the same irradiation patterns than the other samples